An Investigation into the Impact of the Non-integrated and Integrated Sachs-Wolfe Effect on the Analysis of Gravitational Waves

Filip Henriksson
filip@henrikssons.eu

under the direction of
Adam Johansson Andrews
Department of Physics
Stockholm University

Research Academy for Young Scientists
July 14, 2021

Abstract

The purpose of this investigation was to research how gravitational waves are influenced as they propagate through the Universe. The focus was creating an algorithm which predicts the effect of the non-integrated and integrated Sachs-Wolfe effect on gravitational wave frequency, in order to ultimately find the resultant impact on the calculation of chirp mass. This effect is not considered in the LIGO calculation of chirp mass, therefore by analyzing LIGO data from two merger events, GW200115 and GW190521, this investigation aimed to provide a more accurate estimate of the chirp mass of these merger events. Whilst previous literature has attempted to estimate the Sachs-Wolfe effect using a baryonic matter density field, this investigation aims to find a more accurate estimate through being the first to use the BORG dark matter density field together with data from LIGO. The validity of the algorithm was tested using a preliminary baseline test, in which values with known outputs were tested. The results predicted an extremely small increase in frequency, or blueshift, by $1.07 \cdot 10^{-3}\%$ for merger event GW200115. Merger event GW190521 on the other hand resulted in a prediction of a very small decrease in frequency, or redshift, by $1.79 \cdot 10^{-3}\%$. The predicted impact on calculated chirp mass was a magnitude of $10^{-}5$ smaller than the uncertainty provided by LIGO, thus it was concluded that the Sachs-Wolfe effect is much less significant than other sources of uncertainty present in data collection of gravitational waves. The accuracy of the results are difficult to evaluate given that this paper is the first attempt to predict the Sachs-Wolfe effect using a realistic density field. However, as gravitational observatories become more precise, the Sachs-Wolfe effect will become more significant and hopefully more research will be conducted into this area.

Acknowledgements

I would like to acknowledge and thank my mentor Adam Andrews for his support and guidance. I would also like to thank Stockholm University for allowing me to use their facilities at research center AlbaNova. I would like to thank Rays – for Excellence and their partners AstraZeneca and Kjell & Märta Beijers Stiftelse.

Contents

1 Introduction

On the 11th of February 2016 the Laser Interferometer Gravitational Wave Observatory (LIGO) announced together with the Virgo interferometer (VIRGO) the first direct detection of gravitational waves. This monumental breakthrough in experimental physics confirmed Einstein's prediction of gravitational waves proposed in his paper on general relativity 100 years earlier [1]. The observations indicated a merger event between two black holes with 36 and 29 solar masses respectively, in a galaxy more than one billion light years from Earth. The wave power radiated by the gravitational waves during the strongest 0.2 seconds of the merger exceeded the power radiated by all of the stars in the observable Universe. [2]

Since this discovery, more merger events have been detected and greatly assisted the research on gravitational waves, the sources of gravity as well as the structure, dynamics, origin and future of the Universe. Gravitational waves play a crucial role in answering these fundamental questions, thus it is critically important that these waves are analyzed correctly; this includes accounting for how the waves change during their propagation from point of emission to point of observation. Therefore, the aim of this investigation was to quantify how gravitational waves are changed due to intermittent matter as they propagate through the Universe. Specifically, what implications these changes have on the calculation of the chirp mass of the source merger event. This aim was addressed by creating an algorithm which predicts the changes to gravitational waves due to cosmological redshift in addition to the non-integrated and integrated Sachs-Wolfe effect using data from LIGO. In order to understand how the algorithm works and the necessary assumptions which were made, it is vital to understand the relevant cosmological background information. Readers familiar with cosmology including Einstein's field equation, the Friedmann-Lemaître-Robertson-Walker metric, and ΛCDM, can skip forward to section 1.1.2.

1.1 Theoretical Background

This paper will use conventional cosmological units. One of which is the megaparsec (Mpc) which equates to roughly $3.1 \cdot 10^{22}$m and is used to express intergalactic distances. Mass will be expressed in terms of a solar mass units ($M_{\odot}$); one solar mass unit is equal to approximately $2.0 \cdot 10^{30}$kg. [3]

1.1.1 Einstein's Field Equation and the FLRW-Metric

Although earlier physicists had suggested the idea of space being curved, Einstein was the first to link the curvature of space with mass and energy. Einstein demonstrated this link in his field equations which became one of the fundamental governing equations of cosmology. Einsteins field equations express the effect of pressure, $P(t)$, and energy, $\epsilon(t)$, on the metric of spacetime at a certain point and are expressed below in equation 1.1.1,

$\mathrm{R}_{\mu\nu} - \frac{1}{2}R\, g_{\mu\nu} + \Lambda g_{\mu\nu} = \frac{8\pi G}{c^4} T_{\mu\nu}(0)$, where $R_{\mu\nu}$ is the Ricci curvature tensor, R is scalar curvature, $g_{\mu\nu}$ is the metric tensor, Λ is the cosmological constant and $T_{\mu\nu}$ is the energy-momentum tensor. The left side of the equation expresses the curvature and the right side expresses the energy distribution. [4]

Where $R_{\mu\nu}$ is the Ricci curvature tensor, R is scalar curvature, $g_{\mu\nu}$ is the metric tensor, Λ is the cosmological constant and $T_{\mu\nu}$ is the energy-momentum tensor.

However, these equations require knowledge of the precise distribution of mass and energy in the Universe to be able to find the exact shape and curvature of spacetime. Therefore, to utilize Einstein's equations an accurate model of the Universe is required. Friedmann, Lemaître, Robertson and Walker were able to use assumptions about the Universe to design a metric which incorporates the expansion of space and solve Einstein's field equations to fit their model [3]. Friedmann began with two fundamental cosmological assumptions; on astronomical scales of over 100Mpc, the Universe is both homogeneous and isotropic. Homogeneity refers to the Universe being evenly distributed regardless of the location of the observer, thus there are no preferred locations in the Universe [3]. Isotropy means the Universe is uniform and looks the same in all directions. These two assump-

tions combine to form the cosmological principle which states that there is nothing special about our location in the Universe. The cosmological principle is a paramount assumption in cosmology and formed the basis of the Friedmann–Lemaître–Robertson–Walker (FLRW) metric which takes the form shown in equation 1 [3],

$$ds^2 = -c^2dt^2 + a^2(t)[\frac{dx^2}{1 - kx^2/R_0^2} + x^2d\Omega^2] \tag{1}$$

where ds is the comoving distance, dt is the time difference, $a(t)$ is the scale factor, k/R_0^2 denotes the background curvature type and size, and x and Ω are the radial coordinate and solid angle, respectively [3]. The scale factor, $a(t)$, describes how distances in a isotropic and homogeneous Universe expand or contract with time [3]. Moreover, the R_0^2 value refers to the radius of uniformly curved space, which changes according to the scale factor. This model of the Universe allows for only three possible states of curvature: when the dimensionless curvature constant $k = 0$ the Universe is spatially flat, when $k = +1$ the Universe has positive spacial curvature and when $k = -1$ the Universe has negative spatial curvature [3]. In this investigation it is assumed that the Universe is spatially flat as this is currently the most most widely accepted model.

The FLRW metric also leads to the currently widely accepted Lambda Cold Dark Matter (ΛCDM) model, which was used in this investigation. This model outlines the major components of the Universe. Radiation and baryonic matter are previously recognized components, whilst CDM and lambda are postulated by the ΛCDM model [5]. Radiation is energy in the form of photons. The largest source of radiation in the Universe is the Cosmic Microwave Background Radiation which is residual electromagnetic radiation from the Big Bang [5]. Baryonic matter is energy and matter in the form of protons and neutrons. Baryons are subatomic particles made up of three quarks. Cold dark matter (CDM) is an unknown form of matter that has mass and is gravitationally active. Cold refers to matter moving slowly, or non-relativistic compared to light. Dark dark means it only interacts very weakly with the weak and electromagnetic force [5]. Lambda Λ refers

to dark energy which contributes negative pressure to the Universe; dark energy is used to explain the expansion of the universe as the negative pressure results in objects being pushed apart [5]. It is important to note that the universe is not evenly divided into the four components of the ΛCDM model. In fact, dark matter outweighs baryonic matter by roughly five to one [6]. Hence, this investigation makes the valid simplification of using a density field with only dark matter and not baryonic matter. This density field will be explained in more detail in section 2.3.

1.1.2 Gravity and Sachs-Wolfe Effect

On a cosmological scale of more than 100Mpc, the most dominant force governing the motion of objects is gravity and the electromagnetic force is assumed to be negligible [3]. The gravitational force can be viewed from two main perspectives, the Newtonian viewpoint and the Einsteinian, also known as general relativistic, viewpoint. In the Newtonian viewpoint of universal gravitation, all particles exhibit an attractive gravitational force to each other which is proportional to their mass. Einsteinian gravity, however, models gravity as a distortion in the curvature of spacetime due to the presence of matter or energy [3]. This curvature is visualized in 2-dimensions in figure 1 below. The famous quote from John Archibald Wheeler summarizes the relationship well: "Spacetime tells matter how to move; matter tells spacetime how to curve" [7]

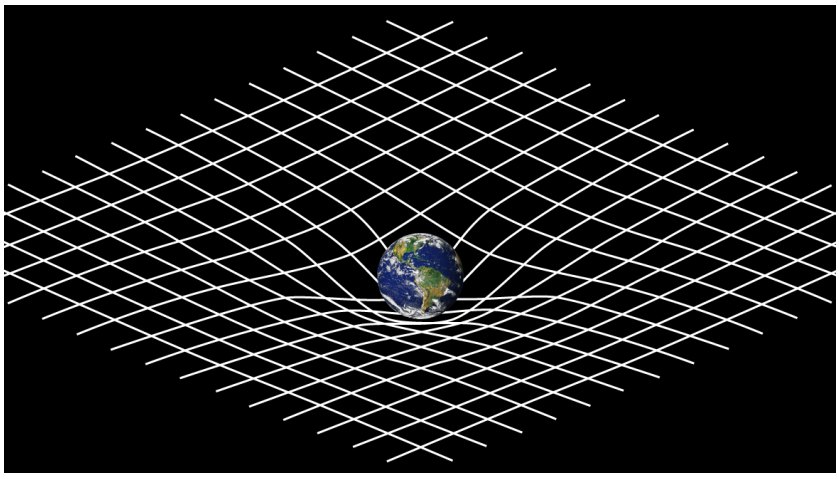

Figure 1: Visualization of spacetime Curvature due to Gravity [8]

In most cosmological contexts the two viewpoints yield very similar predictions, except for situations with very strong spatial curvature in which the Einsteinian viewpoint with general relativity is required for the correct result [3]. In this investigation, the Newtonian viewpoint is used through Poisson's equation.

Friedmann's equations and the general relativistic viewpoint have several key implications. For example, the expansion of space as described in the Friedmanns' equations implies a cosmological redshift to waves propagating through the Universe [9]. This is due to expansion of spacetime causing the wavelength of waves to increase and since the speed of light is constant, the frequency of the wave decreases. Note, this effect is separate from the regular Doppler shift which occurs depending on the relative motion of the emitter and observer.

Another consequence of the expansion of spacetime is called the Sachs-Wolfe Effect. This phenomenon was initially focused on the changes experienced by photons due to gravitational wells in order to explain why the Cosmic Microwave Background radiation (CMB) appears uneven. It was expected that that the CMB would consist of an even distribution of residual radiation from the Big Bang as the Universe has expanded and cooled, however physicists have found varying regions of colder and hotter spots; this apparent inhomogeneity in the CMB is explained by the Sachs-Wolfe effect [3]. Notably, the Sachs-Wolfe effect can also be used to explain similar changes which apply to wave signals as they propagate through the Universe. The non-integrated Sachs-Wolfe effect explains that when a photon or wave enters a gravitational well it gains kinetic energy as gravitational potential energy decreases. Similarly, when the photon or wave exits a gravitational well it loses kinetic energy as gravitational potential energy is gained. As a result, the energy of the photon or wave changes due to the change in potential, causing a change in frequency. This effect considers a static gravitational well and is calculated by measuring the net change in gravitational potential from the point of emission of the signal to the observation point [3]. The integrated Sachs-Wolfe effect on the other hand considers evolving gravitational wells. More specifically, due to the accelerating expansion

of spacetime described in the FLRW metric, the gravitational well stretches as the photon travels [3]. This leads to the gravitational well stretching and the gravitational potential of the well decreasing, hence less energy is expended as the photon leaves the well than the energy gained when the photon entered the well. Consequently, there is a net gain in energy of the photon called a gravitational blueshift as it exits the gravitational well which has been flattened out by the expansion of space-time [3]. The Sachs-Wolfe effect is illustrated in figure 2 below. This effect increases as the Universe gets older, since more gravitational wells form and evolve according to the phenomenon called evolution of large-scale structures [3].

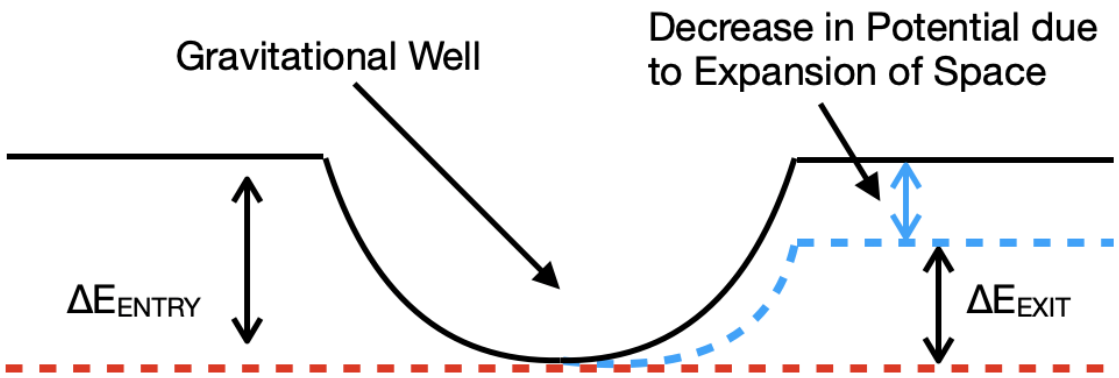

Figure 2: Illustration of the non-integrated Sachs-Wolfe effect (Self-Made).

The integrated Sachs-Wolfe effect sums the change in energy due to the expansion of the universe across all the wells the signal propagates through. Since photons have no mass and travel at the speed of light, an increase in kinetic energy does not refer to speed, but rather the frequency of the photons as seen in equation (2),

$$E = hf, \tag{2}$$

where h is the Plank's constant and f is the frequency of the photon [10].

In summation, there are four main processes in which signals are influenced as they propagate through the Universe: (1) cosmological redshift, (2) regular Doppler shift de-

pending on the motion of the emitter and observer relative to each other and the cosmological flow (3) the Sachs-Wolfe effect which is the net change in energy of the signal due to the difference in gravitational potential from the point of emissions and observer and (4) the integrated Sachs-Wolfe effect which is the change in energy of the signal due to the expansion of the universe and gravitational curvature caused by the intermittent matter [11]. The redshift due to the cosmological expansion will be taken considered in more detail in section 2.1.

The aforementioned uneven appearance of the CMB is known as temperature anistropies ($\frac{\delta T}{T}$) in the cosmic background radiation. Moreover, these anistropies can be mathematically expressed as seen in equation (3) [11],

$$\frac{\delta T}{T} = \Phi_e^r - \vec{n} \cdot \vec{v}_e^r + 2 \int_e^r \partial_\tau \Phi d\lambda \tag{3}$$

,

where $\frac{\delta T}{T}$ is the temperature anistropies for photons, as δT is the net change over the average temperature T. Next, Φ_e^r is the Sachs-Wolfe effect and Φ indicates gravitational potential. The Doppler correction is expressed as $\vec{n} \cdot \vec{v}_e^r$; the source velocity is v and $\vec{n}$ is the unit vector. The integrated Sachs-Wolfe effect is $2 \int_e^r \partial_\tau \Phi d\lambda$; this is an integral along the photon geodesic $d\lambda$ which travels through a changing gravitational potential $\partial_\tau \Phi$ [11]. This fundamental equation will be adapted to this particular investigation in section 2.1.

1.1.3 Black Holes and Gravitational Waves

Gravitational waves are propagating disturbances or "ripples" in the curvature of spacetime, which are formed by moving bodies of immense mass. These waves propagate at the speed of light, c, and all bodies in the path of the wave undergo a tidal gravitational influence which acts perpendicular to the propagation of the wave [12]. For example, when gravitational waves pass through a body such as Earth, the body is minimally stretched and squeezed due to the fluctuation in the fabric of spacetime. LIGO is able to detect this minuscule effect through utilizing lasers, mirrors and extremely sensitive sensors to

detect the tiny changes which the gravitational waves cause in length of two observation arms [13].

Generally the sources of gravitational waves are split into two categories: cosmological origin and relativistic astrophysical origin. Cosmological origin refers to gravitational waves produced in the early stages of the Universe such as during the epoch of inflation and reheating epoch [14]. During these epochs, certain phase transitions occurred such as the symmetric breaking of the grand unification theory, electroweak (EW) phase transition and quantum chromodynamics (QCD) phase transition [14]. Readers that want to read more about these three events are referred to [14]. These phase transitions influence the gravitational waves produced, thus analyzing gravitational waves of cosmological origin can provide significant insight into the physics behind the evolution of the Universe. Gravitational waves of relativistic astrophysical origin are for example those produced by the rotation of non-symmetric neutron stars, explosion of supernovae, inspiral, merger and ringdown of some compact binaries including white dwarfs, neutron stars and/or black holes [14]. This paper will focus on black hole merger events specifically.

Black holes are formed when a star has exhausted the internal thermonuclear fuels in its core; it becomes unstable and collapses inward upon itself. The mass is compressed into a point of virtually zero volume and infinite density known as a singularity [15]. At the singularity, gravity is so strong that nothing, including light can escape. In Einsteinian terms, black holes are an extreme case as at their singularity the curvature of spacetime bends to infinity. Before two black holes merge they undergo a stage called binary black hole inspiral, in which they rapidly orbit around each other. It is during this stage that ripples in the fabric of spacetime known as gravitational waves are generated [14]. This stage is visualized in figure 3:

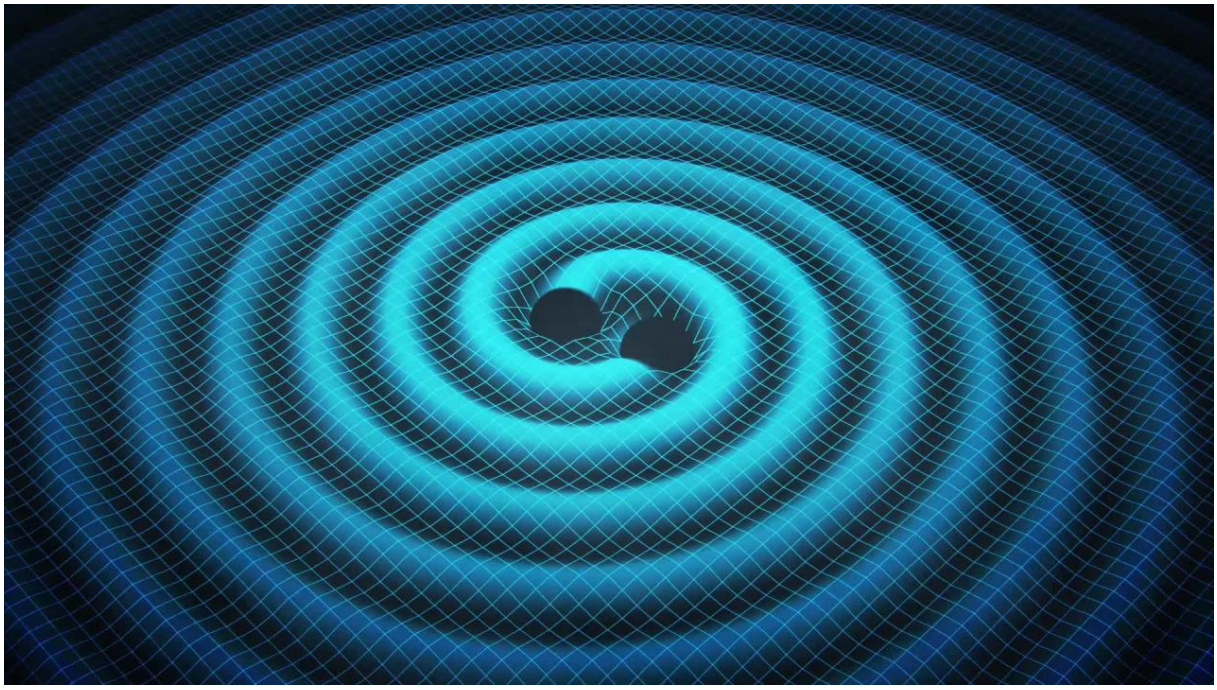

Figure 3: Visualization of black hole inspiral and gravitational wave generation [16]

The final stage is called ringdown and occurs when the black holes finally merge and form a stable state. The formed black hole is of a lower mass than the sum of the previous individual black holes as energy is lost to gravitational and electromagnetic waves. The gravitational waves contain significant information about the nature of the merger and the three individual stages: inspiral, merger and ringdown. For example, in figure 4 which shows a simulated graph of how strain amplitude, h, varies with time, the three stages are clearly distinguishable [17]. The strain amplitude is a measurement of how much a body is stretched or squeezed due to a gravitational wave.

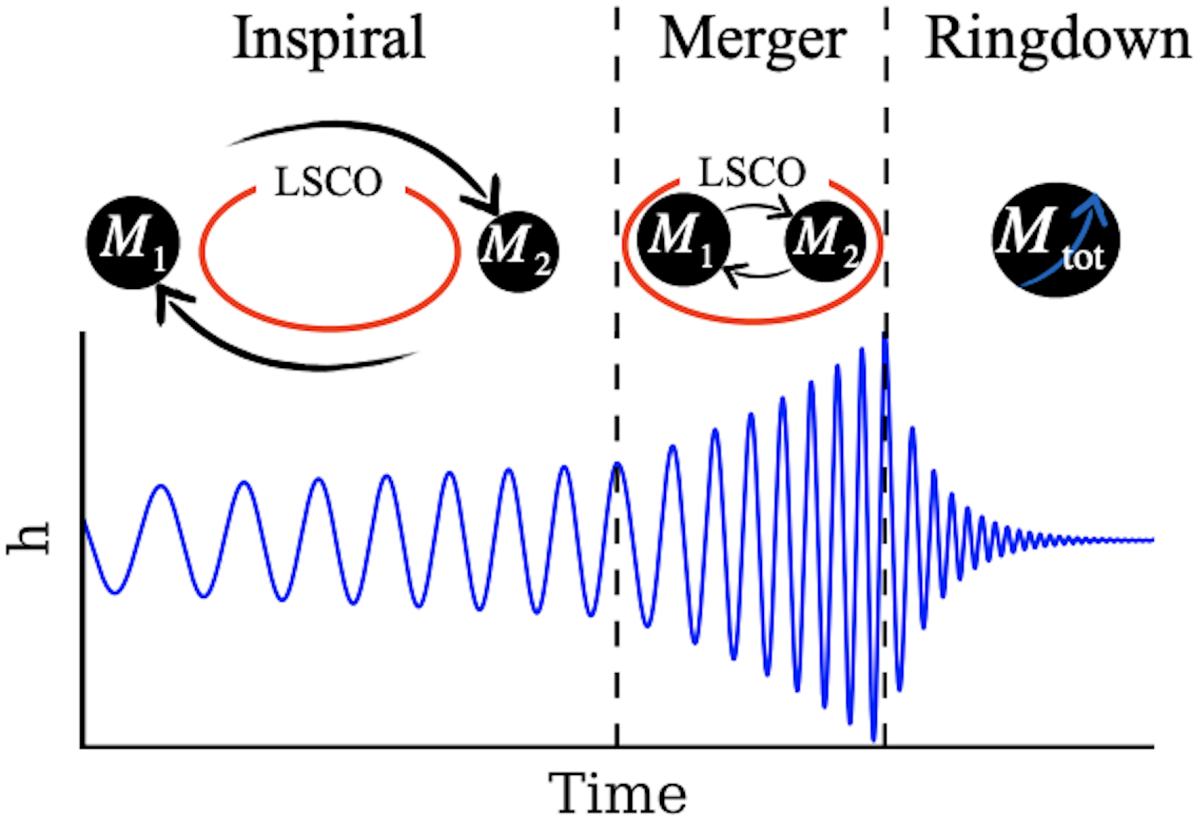

Figure 4: Graph of strain amplitude as a function of time for the inspiral, merger and Ringdown stages of binary black hole coalescence process [17].

There are two key measurements which are essential to the analysis of gravitational waves and will be used in this investigation: chirp mass and luminosity distance. The chirp mass of a black hole merger event is defined as the determinant of the leading-order orbital evolution of the system as a result of energy loss from emitting gravitational waves [18]. This means the orbital frequency of the black holes during the inspiral stage can be mathematically described using chirp mass. The orbital frequency dictates the frequency of the gravitational wave which is emitted by the merger event. The distance from the gravitational wave merger event to the observer is defined as the luminosity distance [18].

In addition to the previously explained four main processes by which wave signals are influenced during propagation mentioned in section 1.1.2, there is also an effect called gravitational lensing. This effect is when signals propagating through the Universe are

bent around large objects due to the curvature of spacetime around these object [3]. Moreover, since black holes are defined as bending spacetime to infinity, information cannot travel through them and is lost; instead this gap is filled by signals which are bent around the black hole. A key simplification in this investigation is that gravitational lensing was not taken into account in the algorithm. Instead, it was assumed that the gravitational waves are only affected by line-of-sight effects.

1.2 Aim of Study

This paper focuses on investigating how gravitational waves are changed due to the non-integrated and integrated Sachs-Wolfe effect. The aim was to provide a more accurate model of these changes than previous literature through using a more realistic simulation of the dark matter density field. The created algorithm with the realistic BORG density field was used to analyze LIGO observations of two separate merger events. The predicted change in frequency of the gravitational waves emitted by the merger events were calculated for the average, maximum and minimum luminosity distances provided by LIGO. These values were then used to determine the significance of the Sachs-Wolfe effect in the calculation of chirp mass of each merger event.

2 Method

First the mathematical method is outlined. Then, the algorithm is explained, as well as the baseline tests which were conducted to test it. Then the data used in the baseline tests is shown and explained; this includes the mock data for the baseline test, LIGO maps for the observational data analysis and the density field used in the algorithm. The results of the baseline test and values generated by the algorithm will be presented in section 3.

2.1 Mathematical Method

The method by which photons propagate through the universe is analogous to gravitational waves. Therefore equation (3), which describes the changes inflicted on photons, can be adapted slightly to describe gravitational waves. Firstly, the combined effect of the Doppler correction, non integrated and integrated Sachs-Wolfe effect can be denoted as χ as seen in equation (4) [11],

$$\chi = \Phi_e^r - \vec{n} \cdot \vec{v}_e^r - I_{ISW}(\lambda_r) \tag{4}$$

where Φ_e^r is the Sachs-Wolfe effect and Φ indicates gravitational potential. The Doppler correction is expressed as $\vec{n} \cdot \vec{v}_e^r$. The source velocity is v and $\vec{n}$ is the unit vector. $I_{ISW}(\lambda_r)$ refers to the integrated Sachs-Wolfe effect which, as explained in equation 3, is equal to $2\int_e^r \partial_\tau \Phi d\lambda$. Then equation (4) can be substituted into equation (5),

$$\frac{f_r}{f_e} = \frac{1-\chi}{1+z} \tag{5}$$

,

to find the change in the frequency emitted (f_e) and frequency received (f_r) [11]. The Doppler correction was set to zero as it is assumed that the source and observer are static in relation to one another. However, the cosmological redshift is significant and is incorporated through the z value in equation (5).

It is important to note that the change in frequency depends on which reference frame is used. Whilst f_e is the emitted signal in the reference frame of the source, the emitted frequency in the observer's reference frame is f_z which is equal to $f_e/(1+z)$ [11]. Thus, we define the change in frequency, Δf, due to the Sachs-Wolfe effect as $\Delta f = f_r - f_z$. Similarly, the change in chirp mass is also defined as $\Delta M = M_r - M_z$, where $M_z = M_e/(1+z)$ [11]. Additionally, since the change in frequency is negatively proportional to the change in the calculation of chirp mass, equation (5) can be rewritten to form equation (6).

$$\frac{\Delta M}{M_z} = \frac{-\Delta f}{f_z} = \chi \tag{6}$$

In summation, the predictions made by the algorithm for the non-integrated and integrated Sachs-Wolfe effect can be used in combination with LIGO data of z to solve for χ and eventually find the change in observed frequency of the gravitational wave and chirp mass of the merger event. The average, maximum and minimum luminosity distances provided by LIGO were all used in order to evaluate the range of possible values for change in frequency and chirp mass.

2.2 Algorithm

The algorithm developed begins with creating a data cube which is a multi-dimensional array of values. The dark matter density field was inserted into the data cube. Mock parameters of a merge event were also inserted, including chirp mass, luminosity distance and astronomical coordinates. Next, the dark matter density field, ρ_m, was translated to the gravitational potential, Φ, through a Fourier transform which simplified the computation. Then the function was inverse Fourier transformed back into spatial coordinates $\Phi(x, y, z)$. The location of the merger event is defined as position "K" and the position of observation is defined as point "O". Next a straight line was drawn between "K" and "O", along which the integrated Sachs-Wolfe effect was calculated using the dark matter density field as seen in equation (7).

$$I_{ISW} = \int_{v_1}^{v_2} \partial_\tau \Phi d\lambda \approx \sum_{O}^{K} \partial_\tau \Phi \Delta\lambda \tag{7}$$

Note, the line does not go perfectly through each voxel, therefore a trilinear interpolation is taken to sum the total Integrated Sachs-Wolfe effect (I_{ISW}) from "K" to "O".

The non-integrated Sachs-Wolfe effect is found by measuring the net change in gravitational potential between "K" and "O". The values for each effect can then be inserted into equations (4) and (5) to find the net change in frequency of the wave. These steps

are summarized in the algorithm flowchart shown in figure 5.

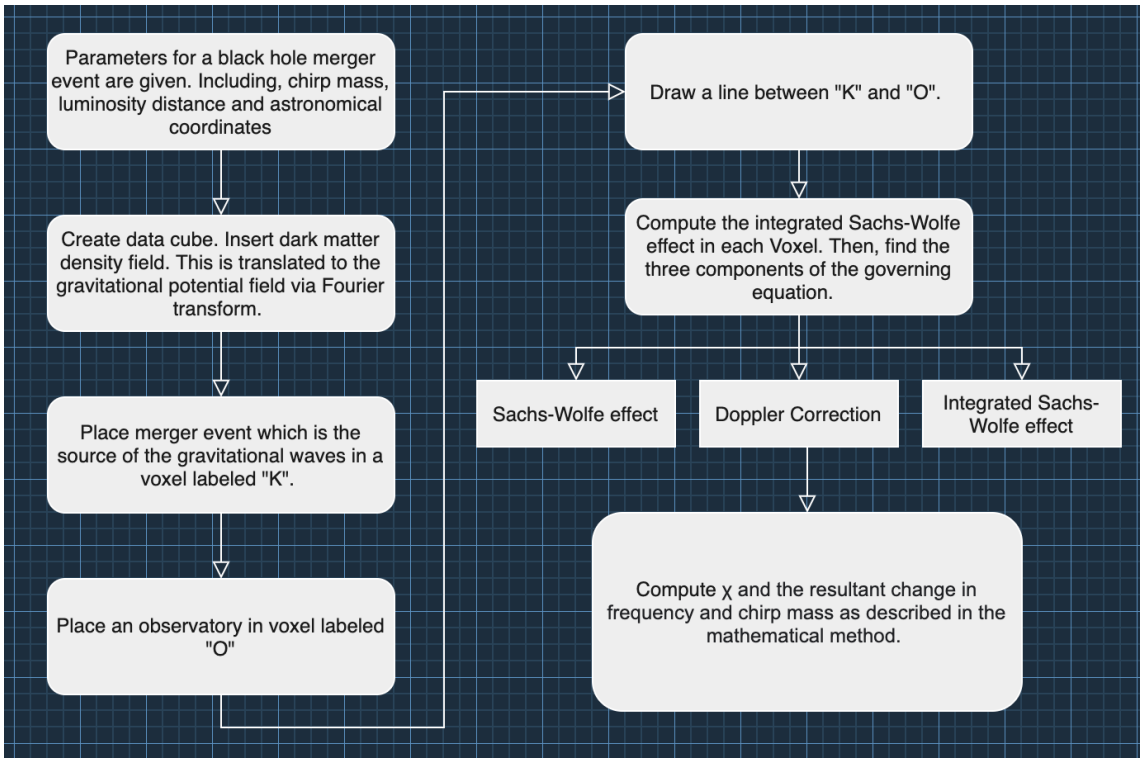

Figure 5: Flowchart of algorithm

2.2.1 Baseline Test

To test the validity of the algorithm a preliminary baseline test was conducted in which certain inputs with known outcomes were run. For the first baseline test, an empty density field was inserted and tested to ensure the value found for the integrated Sachs-Wolfe effect is zero. This outcome was expected as there should be no change in potential as the wave travels through a zero density dark matter field.

Next, a density field with a spherical region of over density around the central observation point was inserted. This input should show one circular region of over density and the rest of the field should be of the same density. Theoretically when the over density field is used, the path of a signal from any point in the universe should experience the same change in potential as the only change in potential occurs when passing through the spherical over density which is the same from all directions. Therefore, a sky map

plot of the integrated Sachs-Wolfe effect from all regions of the universe with the over density field should be a constant color. Moreover, the algorithm should generate a negative value of integrated Sachs-Wolfe effect as the wave is blueshifted through the region of over density as explained in section 1.1.2. The actual outcomes of the baseline test are compared to the expected outcomes in section 3.

2.3 Observational Data

The novel method of analyzing observational data from LIGO involved inserting a BORG dark matter density field into the algorithm. Then, the algorithm together with the dark matter density field was applied to two seprate merger events GW190412 and GW200115

2.3.1 Density Field

The density field used to analyze real world data is often simplified by assuming a Gaussian distribution. This means that there is an equal amount of over and under densities in the field. A slice of this 3D field can be seen in figure 6(a). However, in reality, due to the evolution of large-scale structures, regions of over density and voids become more accentuated over time. Consequently, the Gaussian distribution simplification is limited when analyzing real world data. Instead, a more realistic model is the cosmic density field inferred by the forward modeling algorithm Bayesian Origin Reconstruction from Galaxies (BORG). A slice of the 3D BORG field is shown in figure 6(b).

The BORG algorithm uses models of the formation of gravitational structures to predict the cosmic density field [19]. The cosmic fields generated by the BORG algorithm are constrained by both the physical data model as well as the data from the observed galaxy redshift [20]. This paper uses the density field reconstruction of the Sloan Digital Sky Survey III/Baryon Oscillation Spectroscopic Survey Data Release 12 [19].

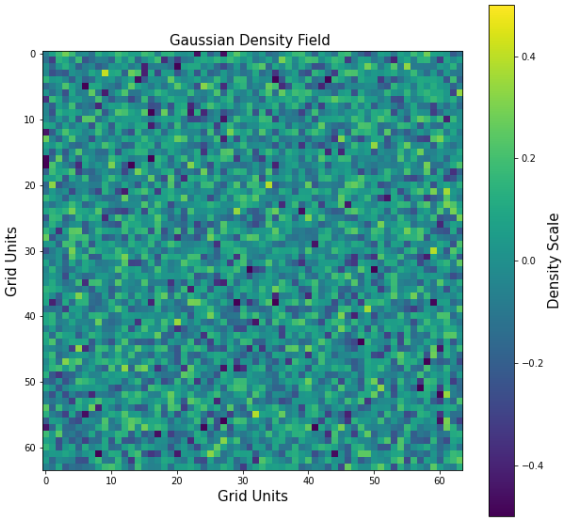

(a) Gaussian distributed density field

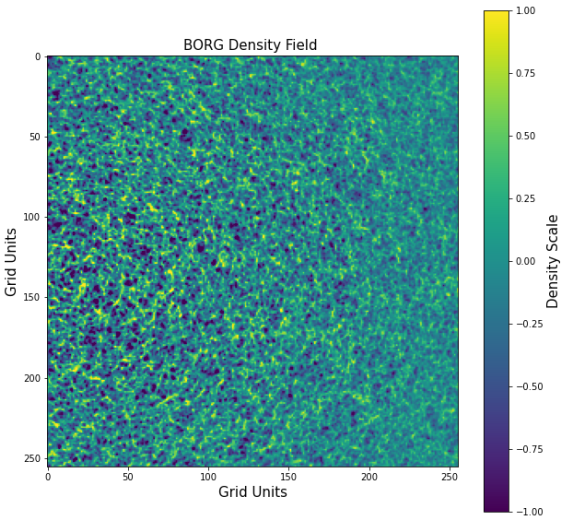

(b) Realistic Simulated field with BORG Algorithm

Figure 6: Comparison of slices of 3D density field models

2.3.2 Merger Event GW200115

The first merger event is GW200115, which was detected by LIGO and VIRGO on January 15th 2020 [21]. In figure 7, a skymap generated from LIGO data of the merger event is shown [21]. This map shows the most probable locations of the origin point of the gravitational wave. These high probability regions are determined through a match-filtering technique, in which random gravitational waves are generated from all direction of the universe and then complex machine learning algorithms match the predictions with the data [22]. This technique can predict what line the wave passes through Earth, however it is difficult to measure from which side of the Earth along this line the wave originated. Therefore, several regions of high probability of the origin of GW200115 can be seen in the skymap.

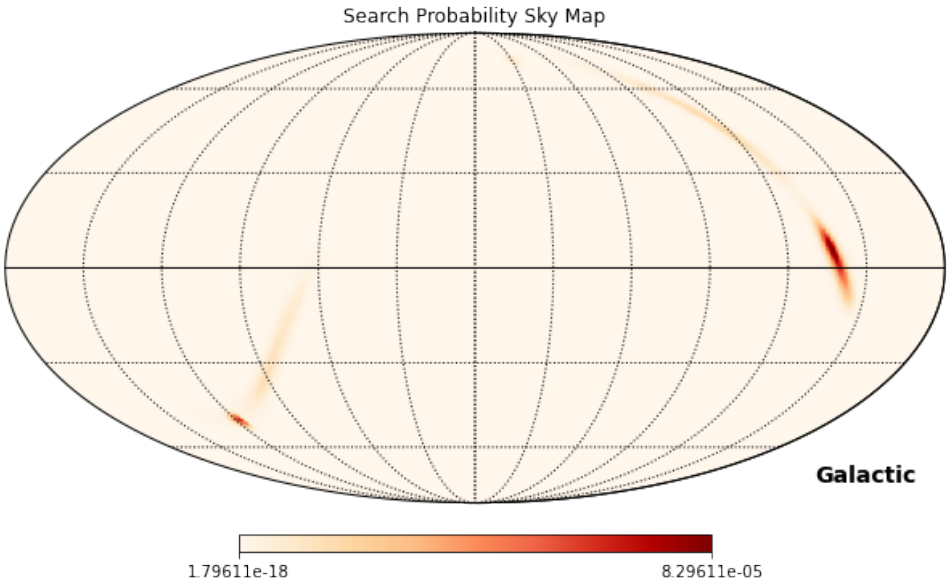

Figure 7: LIGO highest probability region for black hole merger event GW200115 [21]

The probability data shown in figure 7 was inserted into the algorithm and the point of maximum probability was chosen as the point of emission "K" and the center of the density field was chosen as the point of observation "O". In addition to the position of the merger event, the chirp mass and luminosity distance are also required. Data values from LIGO for chirp mass and luminosity distance can be seen in table 1 [21].

Table 1: LIGO Low Spin Merger Data for GW200115

Chirp Mass	$3.41^{+0.08}_{-0.07} M_{\odot}$
Luminosity Distance	280^{+110}_{-110} Mpc

In figure 8, a sky map can be seen of the Integrated Sachs-Wolfe effect on the wave signal produced by a merger event of the characteristics of GW200115 from each point in the Universe. The exact values of the Sachs-Wolfe effect from the exact position of GW200115 are presented in the results section.

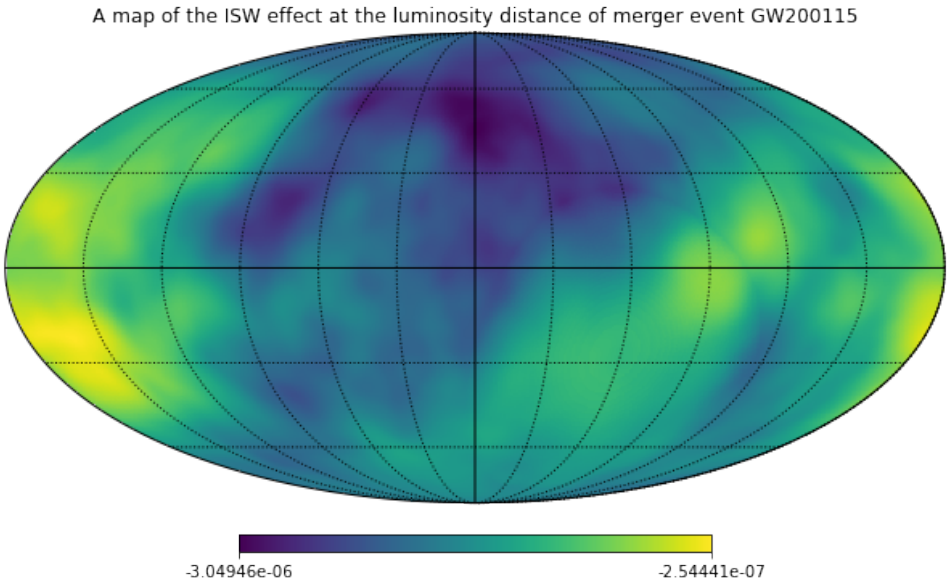

Figure 8: The integrated Sachs-Wolfe effect experienced by a wave signal from the luminosity distance of GW200115 at each point in the Universe.

2.3.3 Merger Event GW190412

The second merger event is GW190412, which was recorded by LIGO and VIRGO on the 12th of April in 2019 [23]. The merger location probability regions can be seen in the skymap in figure 9 below.

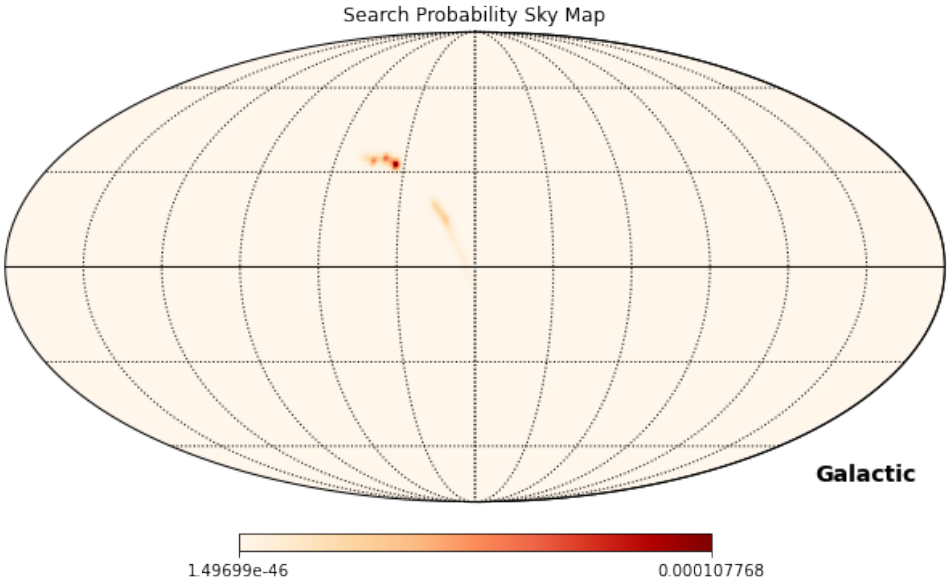

Figure 9: LIGO highest probability region for black hole merger event GW200115 [23].

Moreover, the LIGO data for this meger event is shown in table 2 [23]. .

Table 2: LIGO low spin merger data for GW190412

Chirp Mass	$13.3^{+0.4}_{-0.4} M_{\odot}$
Luminosity Distance	$740^{+130}_{-160} Mpc$

A sky map of the ISW effect on the wave signal produced by a merger event of the characteristics of GW190412 from each point in the Universe is shown below in figure 10.

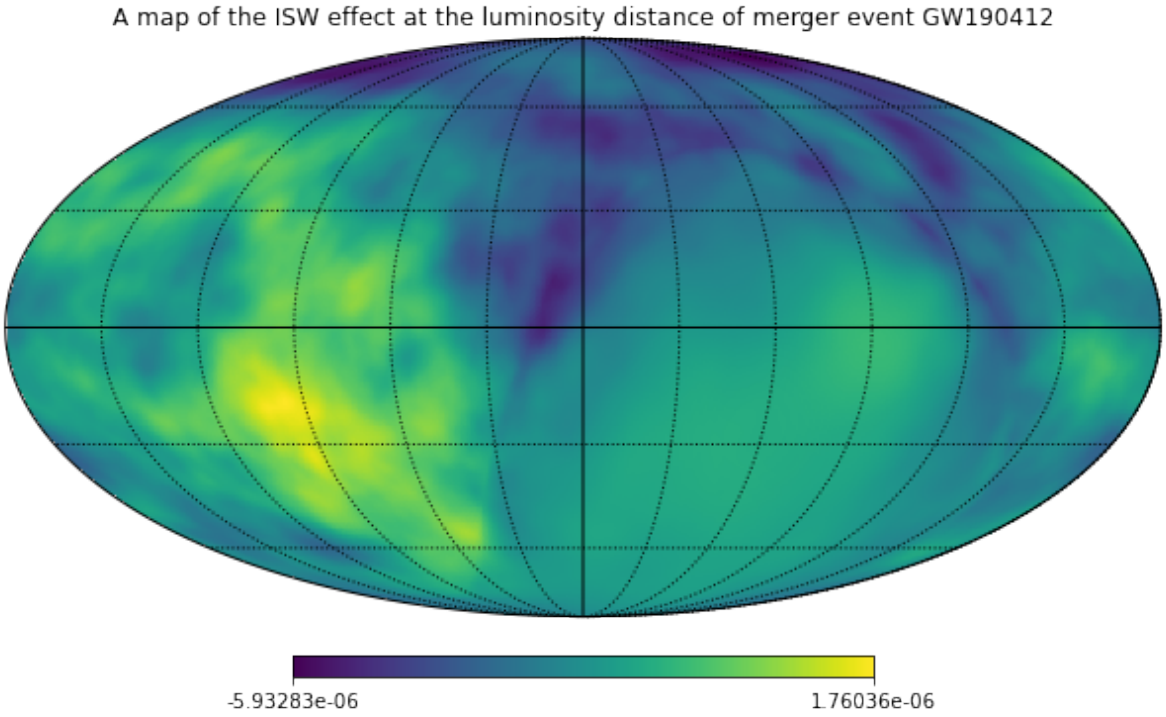

Figure 10: The integrated Sachs-Wolfe effect experienced by a wave signal from the luminosity distance of GW190412 at each point in the universe.

The Sachs-Wolfe effect experienced by a wave signal from the exact position of emission of GW190412, found from figure 9, is presented in the Results section.

In summation, this method allows for an exact pinpoint of the origin of the merger event by analyzing LIGO probability data. Then the algorithm determines the non-integrated and integrated Sachs-Wolfe from the origin to the observer using the average, maximum and minimum luminosity distances provided by LIGO. Then the equations discussed in section 2.1 were used to find the resultant change in frequency, which could

then be used to determine the significance of the Sachs-Wolfe effect on the calculation of chirp mass.

3 Results

First the base line test results were compared to the expected outcomes to validate the algorithm. Then, the results for the merger events are presented as well as the calculated change in frequency and chirp mass.

3.1 Baseline Test Results

The integrated Sachs-Wolfe effect for the model with a zero density field is shown in Figure 11. The sky map shows, using a color spectrum, the magnitude of the integrated Sachs-Wolfe effect signal from each point in the Universe would have due to the inputted density field. As expected, there is no Integrated Sachs-Wolfe effect anywhere as made clear by the constant teal colour.

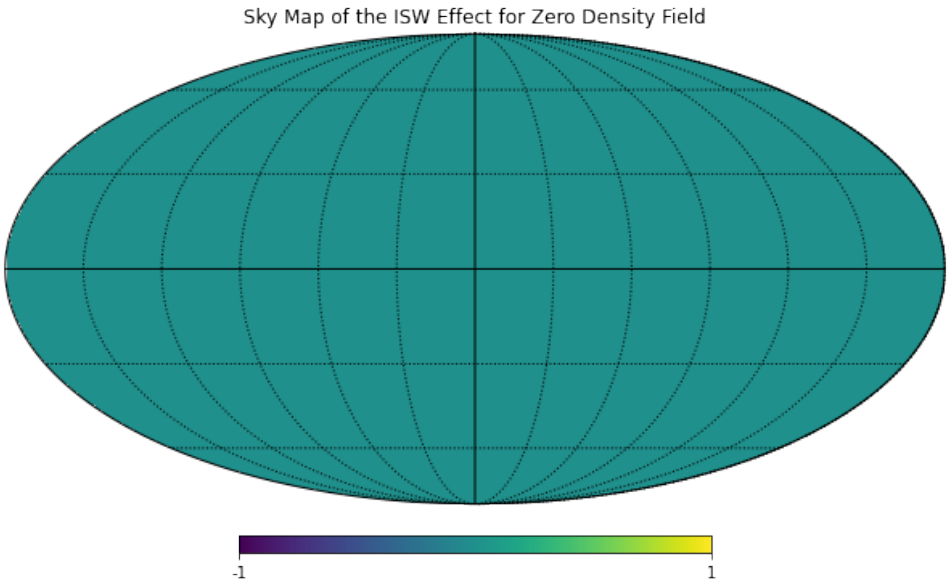

Figure 11: Sky map of integrated Sachs-Wolfe effect for universe modelled with zero density field

Next, the plot of a slice of the 3D over density field is shown in figure 12.

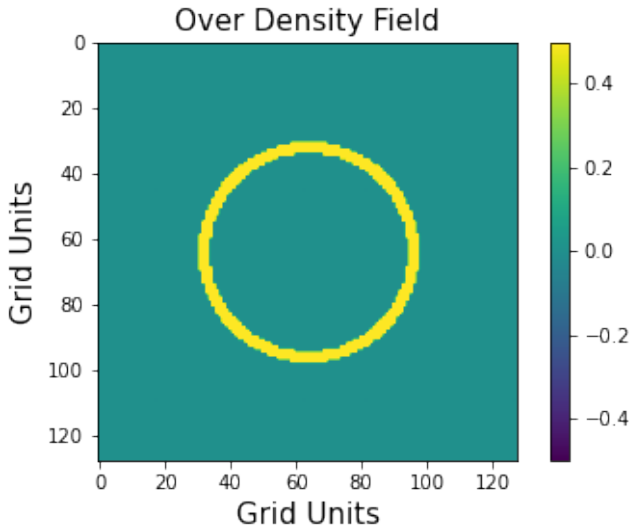

Figure 12: Sliced view of density field with one region of spherical over-density

The plot shows the desired circular region of over density. Moreover, the sky-map of the integrated Sachs-Wolfe effect from each point of the Universe modeled with a spherical region of over density can be seen in figure 13.

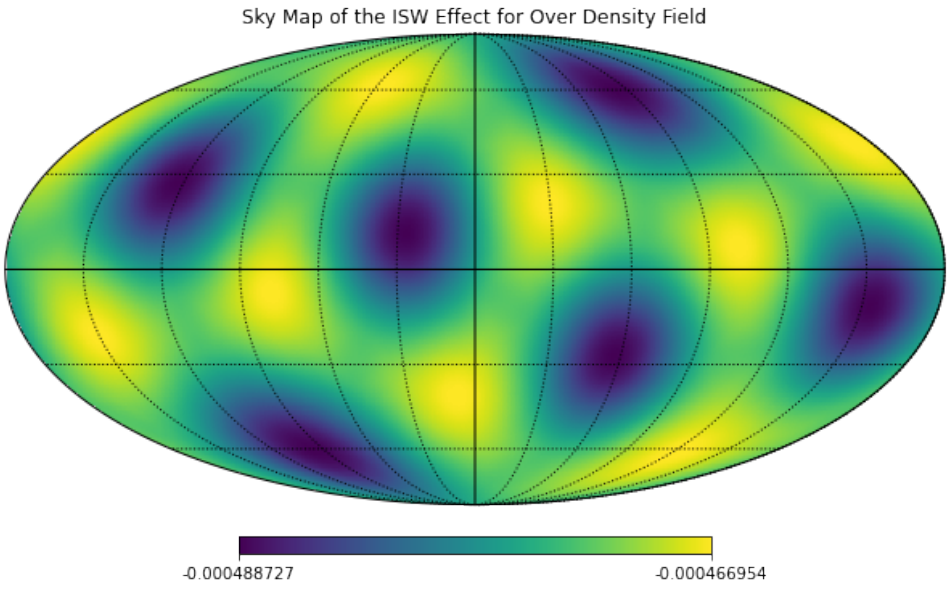

Figure 13: Sky map of integrated Sachs-Wolfe effect for universe modelled with spherical over density field

As mentioned, this sky map should show a constant color as theoretically the integrated Sachs-Wolfe effect should be the same from all directions with the over density

field. However, as made evident by the alternating colours in figure 13, this is not the case. The reason for this is since the algorithm uses cartesian coordinates with square voxels, a perfect spherical region of over density cannot be generated. Consequently the path through some voxels will have a slightly different change in potential than others, resulting in slight variations in the integrated Sachs-Wolfe effect from different parts of the modelled Universe. However, this effect is extremely small, as seen in the scale in figure 13, the variation is in the order of 10^{-5}. A summary of the baseline test results for a mock point is shown in table 3.

Table 3: Baseline test results for mock point source

Density Field	Non-Integrated SW effect (10^{-4})	Integrated SW effect (10^{-4})
Zero Density	0.00	0.00
Over Density	29.1	-4.67

Hence, the baseline test shows the algorithm is valid and can be applied to real world data to predict the significance of the Sachs-Wolfe effect in relation to real gravitational waves.

3.2 Non-integrated and Integrated Sachs-Wolfe Effect

The calculated values for the non-integrated and integrated Sachs-Wolfe effect for merger event GW200115 are shown below in table 4.

Table 4: Algorithm generated values for Non-integrated and Integrated Sachs Wolfe effect for Merger Event GW200115 at Average, Maximum and Minimum Luminosity Distance

Luminosity Distance (Mpc)	SW Effect (10^{-5})	Integrated SW Effect(10^{-7})
(Average) 310	-1.09	-2.54
(Maximum) 460	-0.43	-3.91
(Minimum) 200	-2.61	-1.83

The calculated values for the integrated and non-integrated Sachs-Wolfe effect for merger event GW190521 are shown below in table 5.

Table 5: Algorithm generated values for Non-integrated and Integrated Sachs Wolfe effect for Merger Event GW190521 at Average, Maximum and Minimum Luminosity Distance

Luminosity Distance (Mpc)	SW Effect (10^{-5})	Integrated SW Effect(10^{-7})
(Average) 740	1.91	12.5
(Maximum) 870	-0.072	22.1
(Minimum) 580	0.483	2.6

3.3 Resultant Change in Frequency and chirp Mass

The average, maximum and minimum χ values are shown in table 6 below. The χ values were found with the values presented in table 4 and table 5 using the mathematical method discussed in section 2.1.

Table 6: Average, Maximum and Minimum χ values for each Merger Event

χ Value	GW200115	GW190521
Average χ	-1.07 $\cdot 10^{-5}$	1.79 $\cdot 10^{-5}$
Maximum χ	-3.91 $\cdot 10^{-7}$	-2.93 $\cdot 10^{-6}$
Minimum χ	-1.83 $\cdot 10^{-7}$	4.57 $\cdot 10^{-6}$

Next, the calculated percent change in frequency of the gravitational wave from emission to observation for each merger event is shown below in table 7 and table 8.

Table 7: Average, Maximum and Minimum percentage change in frequency for GW200115

Average Percent Change in Frequency (%)	1.07 $\cdot 10^{-3}$
Maximum Percent Change in Frequency (%)	3.93 $\cdot 10^{-4}$
Minimum Percent Change in Frequency (%)	2.59 $\cdot 10^{-3}$

Table 8: Average, maximum and minimum percentage change in frequency for GW190521

Average Percent Change in Frequency (%)	-1.79 $\cdot 10^{-3}$
Maximum Percent Change in Frequency (%)	2.93 $\cdot 10^{-4}$
Minimum Percent Change in Frequency (%)	-4.57 $\cdot 10^{-4}$

These values for the percentage change in frequency can then be used to find the change in the calculation of chirp mass

Table 9: Change in calculation of Chirp Mass for merger events GW190521

Change in Chirp Mass	GW200115 ($M_\odot$)	GW190521 ($M_\odot$)
Maximum Change	-9.51·10^{-6}	-3.90 ·10^{-5}
Average Change	-2.59·10^{-5}	-2.38·10^{-4}
Minimum Change	-9.51 ·10^{-6}	-3.90 ·10^{-5}

4 Discussion

The final values for the non-integrated and integrated Sachs-Wolfe effect shown in table 4 and table 5 reveal both similarities and differences between how the two merger events were influenced. These variations between the two events are a results of the different regions of density which the two gravitational waves propagated through.

For GW200115 both the non-integrated and integrated Sachs-Wolfe effect were negative for the entire range of possible luminosity distances. As a result, the χ value found was negative for the entire range of possible luminosity distances. This means there was a net blueshift or increase in frequency as explained by equation 4. However, the percent increase in frequency is very small, being in the order of 10^{-3}. The implications of this change can be seen when considering the impact on the calculation of chirp mass. As mentioned, the change in frequency is negatively proportional to the resultant change in the calculation of chirp mass. Therefore, the maximum change in calculated chirp mass is a decrease by $3.93 \cdot 10^{-4}$ % which amounts to a decrease of $9.51 \cdot 10^{-6}$ $M_\odot$. When compared to the value provided by LIGO, 2.42 ± 0.06 $M_\odot$, the change due to the Sachs-Wolfe effect clearly is extremely small.

Merger event GW190521 on the other hand resulted in less consistent values. For the maximum luminosity distance, there is a predicted blueshift with a $2.93 \cdot 10^{-4}$% increase in frequency, whilst for the minimum luminosity distance there is a redshift with a $-4.57 \cdot 10^{-4}$% decrease in frequency. Considering that the average luminosity distance yielded a positive χ value, it is most probable that for this merger event the frequency was redshifted which would lead to a increase in the calculation of chirp mass. However, similar to merger event GW200115, the resultant change in frequency is of a magnitude

of 10^{-4} which is extremely small meaning the change in calculated chirp mass is also extremely small. More specifically, even when using the minimum luminosity distance to find the maximum increase in chirp mass, this increase is still only $6.08 \cdot 10^{-5}\ M_{\odot}$. When compared to the LIGO value for chirp mass, $13.3 \pm 0.4\ M_{\odot}$, the change due to the Sachs-Wolfe effect is extremely small.

It is difficult to critically evaluate the accuracy of the discussed predicted influence of the Sachs-Wolfe effect as this paper is the first estimate of this effect using a realistic density field. However, the predicted changes in chirp mass are well within the margins of uncertainty reported by LIGO. In fact, the significantly larger uncertainties of chirp mass recorded by LIGO suggest other sources of error such as noise from earth and equipment precision are much more significant than the influence of the integrated and non-integrated Sachs-Wolfe effect.

Nevertheless, there are still a few key limitations with predicted values. One limitation with the BORG density field is that it only maps out the dark matter density field. To achieve a closer distribution of the matter distribution, one could also include the baryon matter field and include baryonic effects. However, in the case of the integrated Sachs-Wolfe effect, these effects are relatively minor compared to the effects of the dark matter distribution, since the estimated proportion between dark matter and baryonic matter in the Universe is roughly five to one. Additionally, another key limitation was the assumption that the gravitational waves travel along the line of sight from the point of emission to observation. As mentioned, in reality signals experience gravitational lensing as they propagate through the universe. Therefore, the gravitational waves GW200115 and GW190521 most likely took a different path of propagation than modeled in this investigation.

Despite these limitations, it is evident that the largest uncertainty remains in the data provided by LIGO. As this data becomes more precise, the Sachs-Wolfe effect will become more significant. This limitation is expected to be greatly reduced as plans for new and improved observation equipment are implemented, for example the Laser Interferometer

Space Antenna (LISA) which is planned to be the first space-based gravitational wave detector by using laser interferometry. LISA will have much higher sensitivity to long-period gravitational waves due to the much longer observation "arm" length of 2.5milllion kilometers, compared to LIGO observatory "arm" length of 4 kilometers [13].

4.1 Conclusion

This investigation was able to provide a more realistic approach to estimating the changes in frequency experienced by gravitational waves during propagation through using a more realistic dark matter density field. The results indicated a very small blueshift for merger events GW200115 and a very small redshift for GW190521. Moreover, the predicted change in frequency of these merger events was used to find an estimate of the significance of the Sachs-Wolfe effect on calculating chirp mass. It was concluded that other sources of error during gravitational wave detection present much more significant uncertainties than the influence of the Sachs-Wolfe effect. However, as the gravitational wave observatories become more precise, the Sachs Wolfe effect will become much more relevant.

Improving the accuracy of the analysis of gravitational waves is essential to the advancement of our understanding of the universe. Gravitational waves reveal a unique view of the universe by providing information not available through analysing electromagnetic waves. The study of gravitational waves facilitates an exciting period of research within cosmology and our pursuit of answering fundamental questions concerning the origin, evolution and future of the universe. It is therefore crucial that the analysis of these waves is as accurate as possible.

References

[1] Einstein A. The field equations of gravitation. Sitzungsber Preuss Akad Wiss Berlin (Math Phys). 1915;1915:844–847.

[2] WILL CM. Did Einstein Get It Right? A Centennial Assessment. Proceedings of the American Philosophical Society. 2017;161(1):18–30. Available from: `http://www.jstor.org/stable/45211536`.

[3] Ryden B. Introduction to Cosmology. Introduction to cosmology / Barbara Ryden San Francisco, CA, USA: Addison Wesley, ISBN 0-8053-8912-1, 2003, IX + 244 pp. 2003 01.

[4] Walters S. How Einstein Got His Field Equations. 2016.

[5] of Encyclopaedia TE. black hole. John Wiley & Sons; 2015.

[6] J AP. La materia y la energía oscuras del universo [Dark matter and dark energy of the universe]. Anales de la Real Academia Nacional de Medicina. 2005.

[7] Wheeler JA, Ford K. Geons, black holes and quantum foam: a life in physics. American Association of Physics Teachers; 2000.

[8] Mattson B. 100 Years of General Relativity. NASA. 2015 11.

[9] Durrer R, Maartens R. Dark energy and dark gravity: theory overview. General Relativity and Gravitation. 2008;40(2-3):301–328.

[10] Arons AB, Peppard M. Einstein's Proposal of the Photon Concept—a Translation of the Annalen der Physik Paper of 1905. American Journal of Physics. 1965;33(5):367–374.

[11] Laguna P, Larson SL, Spergel D, Yunes N. Integrated Sachs–Wolfe Effect for Gravitational Radiation. The Astrophysical Journal Letters. 2010;715(1):L12.

[12] Kokkotas KD. Gravitational waves. Acta Phys Polon B. 2007;38:3891–3923.

[13] Aasi J, Abbott B, Abbott R, Abbott T, Abernathy M, Ackley K, et al. Advanced ligo. Classical and quantum gravity. 2015;32(7):074001.

[14] Cai RG, Cao Z, Guo ZK, Wang SJ, Yang T. The Gravitational-Wave Physics. Natl Sci Rev. 2017;4(5):687–706.

[15] Liddle A. An introduction to modern cosmology. Encyclopedia Britannica; 2021.

[16] Cho A. Gravitational waves, Einstein's ripples in spacetime, spotted for first time. Science. 2016 02.

[17] Salcido J, Bower R, Theuns T, McAlpine S, Schaller M, Crain R, et al. Music from the heavens - Gravitational waves from supermassive black hole mergers in the EAGLE simulations. Monthly Notices of the Royal Astronomical Society. 2016 01;463.

[18] Scientific L, collaborations V, Abbott B, Abbott R, Abbott T, Abernathy M, et al. The basic physics of the binary black hole merger GW150914. Annalen der Physik. 2017;529(1-2):1600209.

[19] Lavaux G, Jasche J, Leclercq F. Systematic-free inference of the cosmic matter density field from SDSS3-BOSS data. arXiv preprint arXiv:190906396. 2019.

[20] Jasche J, Wandelt BD. Bayesian physical reconstruction of initial conditions from large-scale structure surveys. Monthly Notices of the Royal Astronomical Society. 2013;432(2):894–913.

[21] Abbott R, Abbott T, Abraham S, Acernese F, Ackley K, Adams A, et al. Observation of gravitational waves from two neutron star–black hole coalescences. The Astrophysical Journal Letters. 2021;915(1):L5.

[22] Raman A. On the Signal Processing Operations in LIGO signals. arXiv preprint arXiv:171107421. 2017.

[23] Abbott R, Abbott T, Abraham S, Acernese F, Ackley K, Adams C, et al. GW190412: Observation of a binary-black-hole coalescence with asymmetric masses. Physical Review D. 2020;102(4):043015.